Crack Determination in Time Domain
via Boundary Integral Equation Method

N. Nishimura, Division of Global Environment Engineering,
Kyoto University, Kyoto 606–01, Japan
(京大・工・環境地球　西村直志)

Summary

An inverse problem of determining the shape of a crack from experiments using a physical quantity governed by the wave equation is considered. This inverse problem is converted into another of minimising a fit-to-data cost function. Powell's variable metric method and a regularised boundary integral equation are used to solve this minimisation problem. Some 2D and 3D examples are presented to test the performance of the proposed method.

Introduction

Assume that a domain D is known to contain a crack S having an unknown shape at an unknown location. We are now interested in determining the geometry of this crack experimentally using a physical quantity u governed by wave equation, as in ultrasonic measurements. In the experiment one illuminates the unknown crack with known incident waves, and measures the time histories of the scattered waves at points far away from S. Our inverse problem then attempts to determine S from the experimental data thus obtained and the homogeneous Neumann condition, or the traction free condition in physical terms, on the faces of the crack. In this paper we shall discuss methods of solving this inverse problem with boundary integral equation methods, which are effective not only in sensitivity analysis [1] and crack problems [2], but in crack determination problems for elliptic differential equations [3] as well.

Crack determination problems have so far been solved numerically via a variety of ways. For example Santosa & Vogelius [4] used FEM to solve a 2D crack determination problem for Laplace's equation. Kubo et al. [5,6] considered a similar problem in 3D; they used BIEM to solve many direct problems with given candidate cracks, and then picked up the one which fits the experimental data the most. Nishimura & Kobayashi [3] also solved a 3D crack determination problem with the help of regularised hypersingular integral equations and a nonlinear programming technique. The method in [3] was later extended to similar problems governed by Helmholtz' equation [7] or wave equation [8]. Tanaka et. al [9] also considered a related inverse problem in elastodynamics.

The objective of this paper is to extend the 2D method of near field data inversion discussed in Furukawa et al. [8] to the far field inversion in 2D and 3D; we believe that the latter is of more practical importance than the former considering the size of cracks found in real structures. Specifically, we consider an infinite domain D containing one single crack S, whose location and shape are unknown. The crack S is determined as a minimiser of a cost function defined as the sum of the squared differences between

computed and measured scattered far fields produced by several known incident waves. The minimisation is performed with the help of a nonlinear programming technique of the quasi-Newton type (Powell's variable metric method), which needs the derivatives of the cost function with respect to shape parameters of the crack. The computations of these derivatives and the cost itself require solutions of hypersingular integral equations, which we propose to solve with a variational approach. This approach uses Galerkin's method for spatial variables and collocation for time. Finally we show several 2D and 3D numerical examples to test the efficiency and robustness of the proposed method.

2. Regularised Integral Equations for Direct and Inverse Problems

We consider 3D problems because the corresponding 2D results are obtained in a straight forward manner. Let S be a smooth piece of curved surface in R^3, bounded by a smooth edge ∂S. Also let the domain D be defined by $D := R^3 \setminus \bar{S}$. In physical terms the surface S represents a crack. The direct crack problem for wave equation is then formulated into the following initial- boundary value problem: Find a solution $u(\boldsymbol{x}, t)$ which satisfies

$$\Delta u - \ddot{u} = 0 \quad \text{in } D \times (t > 0), \qquad u_S|_{t=0} = \dot{u}_S|_{t=0} = 0 \quad \text{in } D,$$

$$\left(\frac{\partial u}{\partial n}\right)^+ = \left(\frac{\partial u}{\partial n}\right)^- = 0 \quad \text{on } S \times (t > 0), \qquad \lim_{x(\in S) \to x_0(\in \partial S)} \varphi(\boldsymbol{x}, t) = 0 \quad \text{for } t > 0,$$

and the radiation condition for u_S, where $u_S(:= u - u_I)$ and u_I are scattered and incident waves, $\dot{}$ is the derivative with respect to time t, the superposed $+ \ (-)$ indicates the limit on S from the positive (negative) side of S, and $\varphi := u^+ - u^-$ is the discontinuity of u across S, or the crack opening displacement. The positive (negative) side of S is the one into which the normal vector $\boldsymbol{n}$ to $S \ (-\boldsymbol{n})$ points. Also, the wave speed has been set equal to 1 with an appropriate scaling.

The solution to this problem is known to possess the following potential representation in $D \times (t > 0)$:

$$u(\boldsymbol{x}, t) = u_I(\boldsymbol{x}, t) + \int_S \int_0^t \frac{\partial G(\boldsymbol{x} - \boldsymbol{y}, t - \tau)}{\partial n_y} \varphi(\boldsymbol{y}, \tau) d\tau dS_y,$$

$$G(\boldsymbol{x} - \boldsymbol{y}, t - \tau) = \frac{\delta(t - \tau - |\boldsymbol{x} - \boldsymbol{y}|)}{4\pi |\boldsymbol{x} - \boldsymbol{y}|}, \tag{1}$$

where $G(\boldsymbol{x} - \boldsymbol{y}, t - \tau)$ is the fundamental solution for the wave equation and $\delta(\cdot)$ is Dirac's delta. The unknown crack opening displacement φ is determined as the solution to the following integral equation:

$$0 = \frac{\partial u_I(\boldsymbol{x}, t)}{\partial n} + \fint_S \int_0^t \frac{\partial}{\partial n_x} \frac{\partial}{\partial n_y} G(\boldsymbol{x} - \boldsymbol{y}, t - \tau) \varphi(\boldsymbol{y}, \tau) d\tau dS_y, \quad (\boldsymbol{x}, t) \in S \times (t > 0) \tag{2}$$

where the integral with a superimposed $=$ denotes an integral in the sense of the finite part.

An effective way of solving the hypersingular integral equation in (2) is to utilise variational formulations in which integration by parts reduces the singularity of kernel functions to integrable one. An attempt of this type has been made by Bécache in [10]

who used the Galerkin method for both spatial variables and time. She found, however, that one has to take the time increment small in order to get a stable numerical result [10]. In this paper we shall use the following variational equation in conjunction with the Galerkin method applied to spatial variables and collocation to time:

$$\int_S e_{\alpha\beta} \frac{\partial \psi(\boldsymbol{x})}{\partial s_\alpha} \frac{\partial x_p(\boldsymbol{x})}{\partial s_\beta} ds_{1_x} ds_{2_x}$$

$$\int_S \int_0^t G(\boldsymbol{x}-\boldsymbol{y}, t-\tau) e_{\lambda\mu} \frac{\partial \varphi(\boldsymbol{y},\tau)}{\partial s_\lambda} \frac{\partial x_p(\boldsymbol{y})}{\partial s_\mu} d\tau ds_{1_y} ds_{2_y}$$

$$+ \int_S e_{ijk} \psi(\boldsymbol{x}) \frac{\partial x_j(\boldsymbol{x})}{\partial s_1} \frac{\partial x_k(\boldsymbol{x})}{\partial s_2} ds_{1_x} ds_{2_x}$$

$$\int_S \int_0^t G(\boldsymbol{x}-\boldsymbol{y}, t-\tau) e_{ipq} \frac{\partial x_p(\boldsymbol{y})}{\partial s_1} \frac{\partial x_q(\boldsymbol{y})}{\partial s_2} \ddot{\varphi}(\boldsymbol{y},\tau) d\tau ds_{1_y} ds_{2_y}$$

$$= \int_S \psi(\boldsymbol{x}) \frac{\partial u_I}{\partial n}(\boldsymbol{x}, t) dS, \tag{3}$$

where $s_{1,2}$ is an arbitrary system of curvilinear coordinates on S, $e_{\alpha\beta}$ and e_{ijk} are 2 and 3 dimensional permutation symbols, and ψ is a test function which vanishes on ∂S. We henceforth assume that Greek indices run from 1 to 2. Our experience shows that this method stays stable even with a relatively large time increment.

The scattered field u_S given by

$$u_S(\boldsymbol{x}, t) = \int_S \int_0^t \frac{\partial G(\boldsymbol{x}-\boldsymbol{y}, t-\tau)}{\partial n_y} \varphi(\boldsymbol{y},\tau) d\tau dS_y$$

approaches asymptotically to

$$\frac{1}{4\pi|\boldsymbol{x}|} u_F(\hat{\boldsymbol{x}}, T; S, u_I)$$

as $|\boldsymbol{x}| \to \infty$ in the direction (viewed from the origin) given by $\hat{\boldsymbol{x}} := \boldsymbol{x}/|\boldsymbol{x}|$. The factor u_F in this formula allows the following expression:

$$u_F(\hat{\boldsymbol{x}}, T; S, u_I) = \int_S \hat{\boldsymbol{x}} \cdot \boldsymbol{n} \; \dot{\varphi}(\boldsymbol{y}, T + \hat{\boldsymbol{x}} \cdot \boldsymbol{y}) dS_y, \tag{4}$$

where T is a time parameter given by $T := t - |\boldsymbol{x}|$. The quantity u_F will be called 'far field' in the rest of this paper.

We next consider the case where the location and shape of S are unknown. To determine S we illuminate the unknown crack with N known incident waves $u_I^n(\boldsymbol{x}, t)$ ($n = 1, \ldots, N$) and measure the resulting far fields in M directions given by $\hat{\boldsymbol{x}}^m$ ($m = 1, \ldots, M$) at $T = T^k$ ($k = K_{n,m}^1, \ldots, K_{n,m}^2$), where $K_{n,m}^1$ and $K_{n,m}^2$ are the first and the last time steps at which the far field is measured. The inverse problem under consideration attempts to reconstruct S from the data thus obtained. We here try to solve this

inverse problem by converting it into another of minimising a certain cost function. The cost function $J(S)$ to be minimised is defined as follows: Given S, solve

$$\fint_S \int_0^t \frac{\partial}{\partial n_x} \frac{\partial}{\partial n_y} G(\boldsymbol{x} - \boldsymbol{y}, t - \tau)\varphi^n(\boldsymbol{y}, \tau)d\tau dS_y = -\frac{\partial u_I^n}{\partial n}(\boldsymbol{x}, t),$$

$$(\boldsymbol{x}, t) \in S \times (t > 0), \quad n = 1, \ldots, N$$

for the unknown φ^n with (3). We then compute the far field u_F by substituting the solution φ^n into (4). The cost $J(S)$ is then defined by

$$J(S) := \frac{1}{2} \sum_{n=1}^{N} \sum_{m=1}^{M} \sum_{k=K_{n,m}^1}^{K_{n,m}^2} \left(u_F(\hat{\boldsymbol{x}}^m, T^k; S, u_I^n) - u_F^0(\hat{\boldsymbol{x}}^m, T^k; u_I^n) \right)^2,$$

where u_F^0 stands for the far field obtained experimentally. With this cost the crack S is determined as a solution to following minimisation problem:

$$\underset{S}{\text{Minimise }} J(S). \tag{5}$$

In practice one may introduce simplifying assumptions on the shape of S and identify S with a finite number of shape parameters. For example a penny shaped crack can be described by 6 parameters. The cost is now a function of these parameters, and the problem in (5) can be solved with nonlinear programming techniques. In this paper we shall use Powell's variable metric method, which belongs to the family of the quasi-Newton methods. Since this method of nonlinear programming requires derivatives of $J(S)$ with respect to shape parameters for S, one has to find an effective way to compute these derivatives. To this end we view S to be an image of a fixed 'reference crack' S_0 via a mapping $\boldsymbol{x} = \boldsymbol{x}(\boldsymbol{X}, \boldsymbol{a})$, $\boldsymbol{x} \in S$, $\boldsymbol{X} \in S_0$, where a_i $(i = 1, \ldots, L)$ are shape parameters for S. The cost $J(S)$ can now be differentiated directly with respect to a_i in a manner similar to taking material derivatives in the large deformation continuum mechanics. Indeed, one has

$$\overset{\triangledown}{J}(S) = \sum_{n,m,k} \left(u_F(\boldsymbol{x}^m, T^k; S, u_I^n) - u_F^0(\hat{\boldsymbol{x}}^m, T^k; u_I^n) \right) \overset{\triangledown}{u}_F(\boldsymbol{x}^m, T^k; S, u_I^n),$$

$$\overset{\triangledown}{u}_F(\boldsymbol{x}, T; S, u_I^n) = \hat{x}_i \int_S e_{ijk} \frac{\partial \overset{\triangledown}{x}_j(\boldsymbol{y})}{\partial s_\alpha} \frac{\partial x_k(\boldsymbol{y})}{\partial s_\beta} e_{\alpha\beta}\dot{\varphi}^n(\boldsymbol{y}, T + \hat{\boldsymbol{x}} \cdot \boldsymbol{y})ds_1 ds_2$$

$$+ \hat{x}_i \int_S n_i \ddot{\varphi}^n(\boldsymbol{y}, T + \hat{\boldsymbol{x}} \cdot \boldsymbol{y})\hat{\boldsymbol{x}} \cdot \overset{\triangledown}{\boldsymbol{y}}dS_y + \hat{x}_i \int_S n_i \overset{\triangledown}{\varphi}^n(\boldsymbol{y}, T + \hat{\boldsymbol{x}} \cdot \boldsymbol{y})dS_y, \tag{6}$$

where $\overset{\triangledown}{}$ stands for the differentiation with respect to one of the shape parameters.

Notice that the quantity φ^n is known when one calculates $\overset{\triangledown}{J}$, because φ^n is already obtained in the evaluation of J, and the evaluation of J always precedes that of $\overset{\triangledown}{J}$ in Powell's variable metric method. Hence all the quantities in (6) are known except for

$\overset{\triangledown}{\varphi}{}^n$. On the other hand one obtains a variational equation for $\overset{\triangledown}{\varphi}{}^n$ as one differentiates (3) with respect to a_i. Indeed, one has

$$\int_S e_{\alpha\beta}\frac{\partial\psi(\boldsymbol{x})}{\partial s_\alpha}\frac{\partial x_p(\boldsymbol{x})}{\partial s_\beta}ds_{1_x}ds_{2_x}$$

$$\int_S\int_0^t G(\boldsymbol{x}-\boldsymbol{y},t-\tau)e_{\lambda\mu}\frac{\partial\overset{\triangledown}{\varphi}{}^n(\boldsymbol{y},\tau)}{\partial s_\lambda}\frac{\partial x_p(\boldsymbol{y})}{\partial s_\mu}d\tau ds_{1_y}ds_{2_y}$$

$$+\int_S e_{ijk}\psi(\boldsymbol{x})\frac{\partial x_j(\boldsymbol{x})}{\partial s_1}\frac{\partial x_k(\boldsymbol{x})}{\partial s_2}ds_{1_x}ds_{2_x}$$

$$\int_S\int_0^t G(\boldsymbol{x}-\boldsymbol{y},t-\tau)e_{ipq}\overset{\triangledown}{\varphi}{}^n(\boldsymbol{y},\tau)\frac{\partial x_p(\boldsymbol{y})}{\partial s_1}\frac{\partial x_q(\boldsymbol{y})}{\partial s_2}d\tau ds_{1_y}ds_{2_y}$$

$$+\int_S e_{\alpha\beta}\frac{\partial\psi(\boldsymbol{x})}{\partial s_\alpha}\frac{\partial\overset{\triangledown}{x}_p(\boldsymbol{x})}{\partial s_\beta}ds_{1_x}ds_{2_x}$$

$$\int_S\int_0^t G(\boldsymbol{x}-\boldsymbol{y},t-\tau)e_{\lambda\mu}\frac{\partial\varphi^n(\boldsymbol{y},\tau)}{\partial s_\lambda}\frac{\partial x_p(\boldsymbol{y})}{\partial s_\mu}d\tau ds_{1_y}ds_{2_y}$$

$$+\int_S e_{\alpha\beta}\frac{\partial\psi(\boldsymbol{x})}{\partial s_\alpha}\frac{\partial x_p(\boldsymbol{x})}{\partial s_\beta}ds_{1_x}ds_{2_x}$$

$$\int_S\int_0^t G_{,k}(\boldsymbol{x}-\boldsymbol{y},t-\tau)(\overset{\triangledown}{x}_k(\boldsymbol{x})-\overset{\triangledown}{x}_k(\boldsymbol{y}))e_{\lambda\mu}\frac{\partial\varphi^n(\boldsymbol{y},\tau)}{\partial s_\lambda}\frac{\partial x_p(\boldsymbol{y})}{\partial s_\mu}d\tau ds_{1_y}ds_{2_y}$$

$$+\int_S e_{\alpha\beta}\frac{\partial\psi(\boldsymbol{x})}{\partial s_\alpha}\frac{\partial x_p(\boldsymbol{x})}{\partial s_\beta}ds_{1_x}ds_{2_x}$$

$$\int_S\int_0^t G(\boldsymbol{x}-\boldsymbol{y},t-\tau)e_{\lambda\mu}\frac{\partial\varphi^n(\boldsymbol{y},\tau)}{\partial s_\lambda}\frac{\partial\overset{\triangledown}{x}_p(\boldsymbol{y})}{\partial s_\mu}d\tau ds_{1_y}ds_{2_y}$$

$$+\int_S e_{ijk}\psi(\boldsymbol{x})\frac{\partial\overset{\triangledown}{x}_j(\boldsymbol{x})}{\partial s_1}\frac{\partial x_k(\boldsymbol{x})}{\partial s_2}ds_{1_x}ds_{2_x}$$

$$\int_S\int_0^t G(\boldsymbol{x}-\boldsymbol{y},t-\tau)e_{ipq}\ddot{\varphi}^n(\boldsymbol{y},\tau)\frac{\partial x_p(\boldsymbol{y})}{\partial s_1}\frac{\partial x_q(\boldsymbol{y})}{\partial s_2}d\tau ds_{1_y}ds_{2_y}$$

$$+\int_S e_{ijk}\psi(\boldsymbol{x})\frac{\partial x_j(\boldsymbol{x})}{\partial s_1}\frac{\partial\overset{\triangledown}{x}_k(\boldsymbol{x})}{\partial s_2}ds_{1_x}ds_{2_x}$$

$$\int_S\int_0^t G(\boldsymbol{x}-\boldsymbol{y},t-\tau)e_{ipq}\ddot{\varphi}^n(\boldsymbol{y},\tau)\frac{\partial x_p(\boldsymbol{y})}{\partial s_1}\frac{\partial x_q(\boldsymbol{y})}{\partial s_2}d\tau ds_{1_y}ds_{2_y}$$

$$+\int_S e_{ijk}\psi(\boldsymbol{x})\frac{\partial x_j(\boldsymbol{x})}{\partial s_1}\frac{\partial x_k(\boldsymbol{x})}{\partial s_2}ds_{1_x}ds_{2_x}$$

$$\int_S\int_0^t G_{,l}(\boldsymbol{x}-\boldsymbol{y},t-\tau)(\overset{\triangledown}{x}_l(\boldsymbol{x})-\overset{\triangledown}{x}_l(\boldsymbol{y}))e_{ipq}\ddot{\varphi}^n(\boldsymbol{y},\tau)\frac{\partial x_p(\boldsymbol{y})}{\partial s_1}\frac{\partial x_q(\boldsymbol{y})}{\partial s_2}d\tau ds_{1_y}ds_{2_y}$$

$$+\int_S e_{ijk}\psi(\boldsymbol{x})\frac{\partial x_j(\boldsymbol{x})}{\partial s_1}\frac{\partial x_k(\boldsymbol{x})}{\partial s_2}ds_{1_x}ds_{2_x}$$

$$\int_S\int_0^t G(\boldsymbol{x}-\boldsymbol{y},t-\tau)e_{ipq}\ddot{\varphi}^n(\boldsymbol{y},\tau)\frac{\partial\overset{\triangledown}{x}_p(\boldsymbol{y})}{\partial s_1}\frac{\partial x_q(\boldsymbol{y})}{\partial s_2}d\tau ds_{1_y}ds_{2_y}$$

$$+\int_S e_{ijk}\psi(\boldsymbol{x})\frac{\partial x_j(\boldsymbol{x})}{\partial s_1}\frac{\partial x_k(\boldsymbol{x})}{\partial s_2}ds_{1_x}ds_{2_x}$$

$$\int_S \int_0^t G(\boldsymbol{x}-\boldsymbol{y}, t-\tau) e_{ipq} \ddot{\overset{\triangledown}{\varphi}}{}^n(\boldsymbol{y},\tau) \frac{\partial x_p(\boldsymbol{y})}{\partial s_1} \frac{\partial \overset{\triangledown}{x}_q(\boldsymbol{y})}{\partial s_2} d\tau ds_{1_y} ds_{2_y}$$

$$= \int_S \psi(\boldsymbol{x}) u^n_{I,il}(\boldsymbol{x},t)\overset{\triangledown}{x}_l(\boldsymbol{x}) n_i(\boldsymbol{x}) dS + \int_S \psi u^n_{I,i}(\boldsymbol{x},t) e_{ijk} e_{pqk} n_p \frac{\partial \overset{\triangledown}{x}_j(\boldsymbol{x})}{\partial x_q} dS. \qquad (7)$$

One can now solve (7) numerically for $\overset{\triangledown}{\varphi}{}^n$ using the same technique as in (3). See the next section for the detail. In the special case of a penny shaped crack (3) and (7) simplify considerably. The result of this simplification, however, is omitted because of the space limitation.

3. Numerical Techniques

This section outlines the numerical techniques used to obtain the results to be shown in the next section.

1. Discretisation In 3D (3) is solved easily with the Galerkin method applied to space variables and collocation to time. Namely, we substitute Ω^A for ψ and $\sum_B \Omega^B \varphi^{n,B}(t)$ for φ^n in (3), where Ω^A is a shape function on S, and $\varphi^{n,A}(t)$ is the time variation of φ^n at the Ath node on S. The time function $\varphi^{n,A}(t)$ is further discretised with piecewise linear interpolation functions, and the resulting equation is solved with collocation. As regards Ω^A we follow Nedelec [11] to use ordinary piecewise linear triangular elements neglecting the near tip singularity of φ^n. In the discretised version of (3) thus obtained we compute time integrals analytically, and the inner (outer) surface integrals analytically (numerically). Notice that the discretised equations obtained from (7) and (3) are the same if one uses the same shape functions for $\overset{\triangledown}{\varphi}{}^n$ and φ^n. Hence one constructs and triangular-decomposes this matrix equation only when one computes J and reuses the results in the calculation of $\overset{\triangledown}{J}$.

2. Time Increment The choice of the time increment Δt has to be made very carefully in the present analysis because the ratio $\Delta t/$(element size) has an influence on the numerical accuracy of the solution, and because the size of the crack changes during the minimisation. One might possibly adjust Δt according to the current crack size, but this would make the algorithm too complicated. We therefore chose to keep Δt constant in the whole nonlinear programming process. In practice, one may set Δt to be sufficiently small in comparison with the time scale of the variation of the experimental far field data.

3. Time Steps Suppose that one calculates φ for K time steps with a fixed Δt. Equation (4) then shows that one can determine the associated far field for K time steps. In evaluating $J(S)$ one has to compute far fields from a candidate crack at $T = T^k = k\Delta t$ for $k = K^1_{n,m},\ldots,K^2_{n,m}$. Now suppose $K^2_{n,m} = K^1_{n,m} + K - 1$, which is a natural choice. If $T^{K^1_{n,m}}$ is smaller than the computed arrival time T^{K_a} from the candidate crack, there is no problem in the evaluation of the cost function. If $T^{K^1_{n,m}} > T^{K_a}$, however, one may have to increase the number of time steps to compute far fields for $T > T_0$, where $T_0 := (K_a + K - 1)\Delta t$. However, this 'variable K' approach is inconvenient because it may possibly make the computational time uncontrollable. We therefore decided to keep the number of time steps K constant in the calculation of u_F, and set $u_F(\cdot,T;\cdot,\cdot)$ equal to $u_F(\cdot,T_0;\cdot,\cdot)$ for $T \geq T_0$.

4. Numerical Examples

This section shows a few 2D and 3D numerical examples. We here try inversions of numerically simulated experimental data, rather than real ones. For the simulation we used BIEM with the true crack geometry, and gave noise to the computed far field, thus producing input data to the inverse problem solver. The number of time steps is 15 in all the examples.

1. 2D Problems The crack is assumed to be a straight line, which we can identify by 4 shape parameters, i.e. $x_{1,2}$ coordinates of the tips. We consider two incident waves given by $u_f^n = f(t - t_n - x_n)$, $(n = 1, 2)$, where t_n is a certain number chosen so that the incident wave does not reach the crack at $t = 0$, $f(\cdot)$ is defined by

$$f(t) = \begin{cases} 1 - \cos \frac{t}{l} & 0 \le t \le 2\pi l \\ 0 & \text{otherwise} \end{cases}, \tag{8}$$

and $l = 2$. For the crack we used 9 piecewise linear boundary elements, and the time increment is 1.5 times the average element size in the true crack. The directions of far field measurements are $\hat{x}^m = (\cos\theta^m, \sin\theta^m)$ with $\theta^{1,2,3,4} = 45°, 135°, -45°, -135°$, and 30% of random error is given to the data. Each tip is constrained to stay within a circle having a radius of 3 centred at the origin, in order to avoid divergence of the solution. Fig. 1 shows the true crack, initial guess and the intermediate crack locations at each evaluation of J in the minimisation process. As this figure shows the analysis converged to a crack sufficiently close to the true one. The CPU time was about 2 sec. on Fujitsu M1800 (a scalar processor).

2. 3D Problems The crack is assumed to be penny shaped, and is illuminated by three incident waves given by $u_f^n = f(t - t_n - x_n)$ $(n = 1, 2, 3)$ with $l = 1$, see (8). We use 6 shape parameters for the crack as in [3], and 21 piecewise linear shape functions for unknowns on S. The time increment is set equal to the average element length in the radial direction of the true crack. The far field measurement is made in 14 directions, which consist of $\pm$ the coordinate directions (6 directions) and $(\pm 1/\sqrt{3}, \pm 1/\sqrt{3}, \pm 1/\sqrt{3})$ (8 directions). The data is noisy with 20% of random error. Fig. 2 shows the true crack, initial guess and the intermediate crack locations at each evaluation of J. As this figure shows the analysis converged to a crack sufficiently close to the true one. The CPU time was about 45 sec. on Fujitsu VP2600 (a vector processor).

5. Concluding Remark

The method discussed in this paper can easily be extended to elastodynamics. An investigation along this line is now under way.

References

1. Barone, M.R.; Yang, R.-J.: Boundary integral equations for recovery of design sensitivities in shape optimization. AIAA J. **26** (1988) 589–594.
2. Nishimura, N.; Kobayashi, S.: A regularized boundary integral equation method for elastodynamic crack problems. Comp. Mech. **4** (1989) 319–328.
3. Nishimura, N.; Kobayashi, S.: A boundary integral equation method for an inverse problem related to crack detection. to appear in Int. J. Num. Meth. Eng. (1991).
4. Santosa, F.; Vogelius, M.: A computational algorithm to determine cracks from electrostatic boundary measurements. Int. J. Eng. Sci. **29** (1991) 917–937.

38

5. Kubo, S.: Inverse problems related to the mechanics and fracture of solids and structures. JSME Int. J. **31** (1988) 157–166.

6. Sakagami, T.; Kubo, S.; Ohji, K.; Yamamoto, K.; Nakatsuka, K.: Identification of a three-dimensional internal crack by the electric potential CT method. Trans. JSME **56** (1990) 27–32 (in Japanese).

7. Nishimura, N.: Regularised integral equations for crack shape determination problems. Inverse Problems in Engineering Sciences (Eds. M. Yamaguti et al.), Springer, (1991) 59–65.

8. Furukawa, A.; Nishimura, N.; Kobayashi, S.: Crack determination by time-domain BIEM. Proc. BTEC (1991) 67–70 (in Japanese).

9. Tanaka, M.; Nakamura, M.; Nakano, T.: Detection of cracks in structural components by the elastodynamic boundary element method. Proc. BEM12, Comp. Mech. Publ., **2** (1990), 413–424.

10. Bécache, E.: Doctoral Thesis. Université de Paris VI, (1990).

11. Nedelec, J.C.: Integral equations with non integrable kernels. Integral Eq. Operator Th. **5** (1982) 562–572.
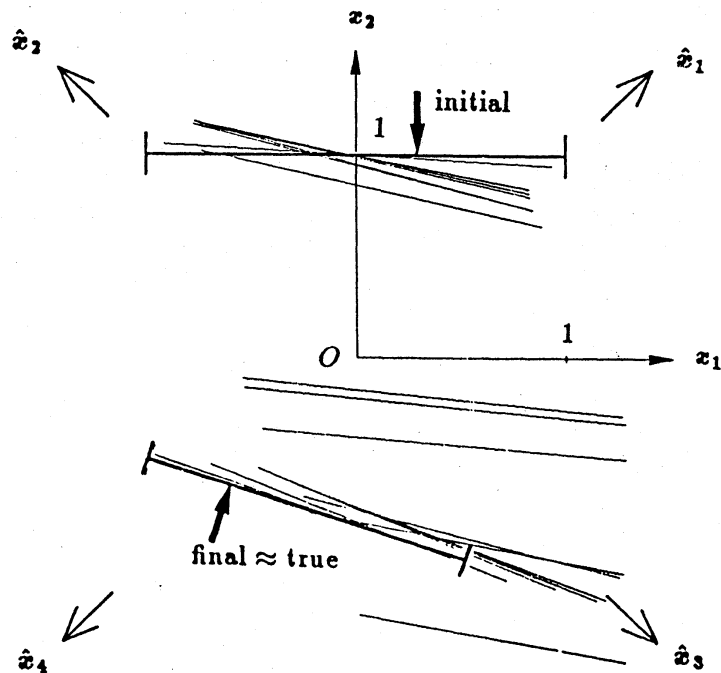
Fig. 1 Mode of convergence in 2D crack determination analysis in time domain.
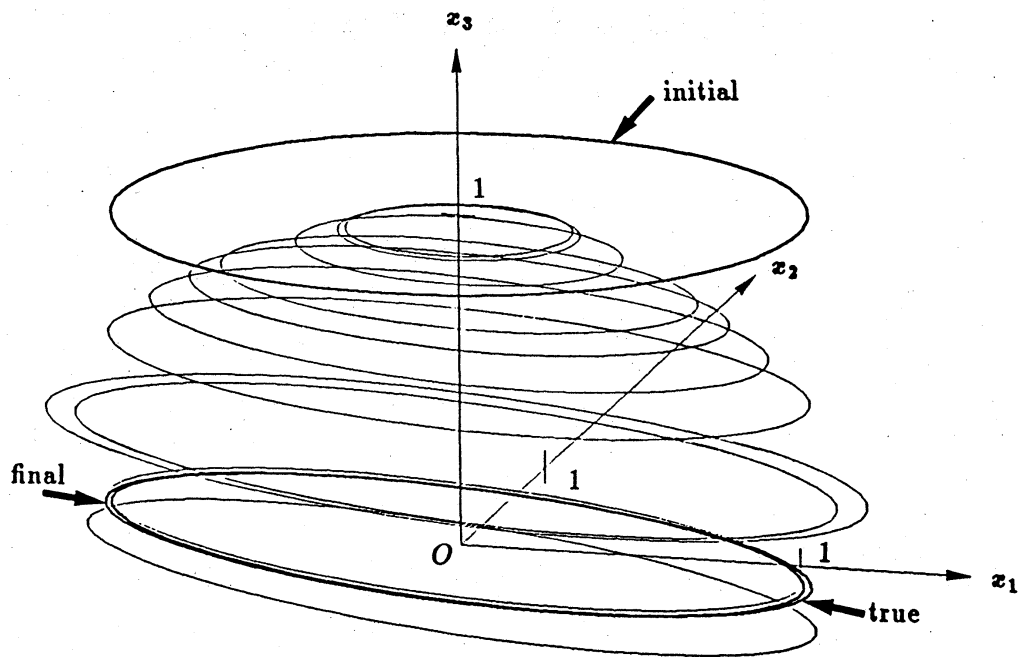
Fig. 2 Mode of convergence in 3D crack determination analysis in time domain.